Journal of Natural Sciences and Mathematics
Qassim University, Vol. 10, No. 1, pp 1-26 (January 2017/Rabi II 1437H.)

Synthesis, Spectroscopic Characterization and Antimicrobial Activity of Novel Azo-acetohydrazide Metal Complexes

Ahmed N. Al-Hakimi [1,2], Fathy A. Elsaied,[3] Mohamad M.E. Shakdofa[4,5],
Samir O. M. Al asbahi[6], I. A. Alhagri[1,2]
Ashwaq M. A. Alkwlini[2], Mohammed A. Wahba[5]

[1]Faculty of Science, Chemistry Department, Qassim University, Qassim, Saudi Arabia (KSA)

[2]Faculty of Science, Chemistry Department, Ibb University, Ibb, Yemen,

[3]Department of Chemistry, Faculty of Science, El-Menoufia University, Shebin El-Kom, Egypt

[4]Faculty of Sciences and Arts, Chemistry Department, Khulais, University of Jeddah, Saudi Arabia

[5]National Research Centre, Inorganic Chemistry Department, Dokki, Cairo,

[6]Faculty of Science, Physics Department, Ibb University, Ibb, Yemen

Abstract. A novel azo-ligand was synthesized by condensation of 2-hydroxy-5-(*p*-tolyldiazenyl) benzaldehyde, with 2-(phenylamino) acetohydrazide. The ligand as well as its complexes have been characterized by various spectroscopic and analytical techniques. The spectral data confirmed that the ligand adopted either a neutral bidentate or a dibasic tridentate mode, bonded to the metal ions through the oxygen atom of the carbonyl group, azomethine nitrogen atom and/or deprotonated phenolic oxygen atom forming either a tetragonally distorted octahedral, an octahedral or a square planer geometry. X-ray powder diffraction analysis of complexes **$[Cu(H_2L)_2Cl_2].2H_2O$** and **$[Cu(L)(H_2O)_3]$** indicated that the complexes are crystalline in nature and have monoclinic structures. The antibacterial as well as the antifungal activities of the ligand and its complexes were evaluated against *Escherichia coli* and *Aspergillus niger* by well- diffusion method. The results showed that complex **$[VO(H_2L)_2(SO_4)]H_2O$** exhibits the highest antifungal activity while complex **$[Cu(L)(H_2O)_3]$** exhibits the highest antibacterial activity among the tested complexes.

***KeyWords*:** Azohydrazone, acetohydrazide, metal complexes, bioactivity, XRD

1. Introduction

Hydrazine and hydrazone compounds are a category of Schiff base compounds with N-N linkage. They have drawn a significant interest to medicinal chemical researchers for several years, because of their varied biological and pharmaceutical implementations. Among these implantations, metal complexes of hydrazine showed pronounced activities as: antimicrobial,[1, 2] antibacterial,[1, 3-5] antifungal[1, 5] anticancer,[6-9] anticandidal,[6] anti-tubercular,[10, 11] analgesic, anti-inflammatory[12], anticonvulsant[13] and leishmanicidal[14, 15] compounds. The literature scope of these compounds revealed their promising activities in treatment of certain diseases. N-2-(4-benzylpiperidin-/piperazin-1-yl) acylhydrazone derivatives was tested in treatment of Alzheimer diseases. They showed a promising ability to inhibit acetylcholinesterase, butyrylcholinesterase and aggregation of amyloid beta peptides.[16]

Shabbir et. al. studied the anti-arthritic activity of 2,4-dihydroxyphenyl acetohydrazide derivatives. They reported a significant anti-arthritic activity of these compounds which may be assigned to immunomodulatory and anti-inflammatory effects.[17] The inhibitory effects of end-to-end thiocyanato-bridged zig-zag polymers of Cu(II), Co(II) and Ni(II) complexes with tridentate hydrazone ligand on the cell viability of human lung carcinoma cells (A549 cells), human colorectal carcinoma cells (COLO 205 cells and HT-29 cells), were reported[18]. Among the tested compounds, $[Cu(LH)(NO_3)(l1,3\text{-}NCS)]_n.nH_2O$ had the strongest population growth inhibition of human colorectal carcinoma cells (COLO 205 cells and HT-29 cells).[18] The anti-inflammatory and analgesic activity of Cu(II) and Zn(II) complexes of 2-(naphthalen-1-yloxy)-N-(1-(pyridin-2-yl) ethylidene) acetohydrazide have been tested and compared with piroxicam. All tested compounds recorded a remarkable anti-inflammatory and analgesic effect in comparison to piroxicam[19]. The antiamoebic activity of 2-(quinolin-8-yloxy) acetohydrazide metal complexes have been reported, The results demonstrated a promising antiamoebic activity of some complexes. On the other hand the toxicological studies of these compounds on human breast cancer MCF-7 cell line showed that all tested compounds and metronidazole were nontoxic at the concentration range of 1.56- 50 mM[20] From another point of view, hydrazone ligands derivatives have been employed as extracting agents in spectrophotometric determination of some ions[21] and species in pharmaceutical formulations[22] as well as its wide scope of application in the in the catalytic[23] and wastewater treatment processes.[24] In view of the above multiple growing importance of these compounds, we report the synthesizing of new azo-hydrazone ligand derived by condensation of 2-hydroxy-5-(p-tolyldiazenyl) benzaldehyde with 2-(phenylamino) acetohydrazide, the work includes also synthesizing Zn(II), Cu(II), Ni(II), Co(II), Mn(II), Fe(III), Ru(III) and VO(II) complexes of this ligand. All compounds were characterized using analytical techniques such as elemental and thermal analyses, molar conductance, magnetic susceptibility measurements, X-ray diffraction as well as spectroscopic

techniques such as UV-Visible, IR, ^{1}H and ^{13}C-NMR. The research was extended to evaluate the microbicidal activities of the ligand and its complexes.

2. Experimental

2.1. Materials

All reagents employed for the preparation of the ligands and their complexes were of the analytical grade available and used without further purification. 2-hydroxy-5-(*p*-tolyldiazenyl) benzaldehyde, and 2-(phenyl amino) acetohydrazide were prepared according to published methods[25, 26]. DMSO (assay 99.7%); absolute ethanol (assay ≥ 99.8 %) were used. Metal salts were provided from SIGMA-ALDRICH Company (purity from 98% to 99.99%). The purity of all prepared compounds was confirmed by TLC.

2.2. Instrumentation and measurement

Elemental analysis (CHN) was performed in the Analytical Unit, Cairo University (Egypt) by the usual methods of analysis. Standard analytical methods were used to determine the metal ion content [27-29]. IR spectra of the solid ligand and complexes were recorded on a Perkin Elmer 681 and Perkin Elmer 1430 spectrometer as KBr pellets. The ^{1}H- and ^{13}C-NMR spectra were recorded with a JEOL JNM-ECP-400 MHz FT-NMR spectrometer in d_6-DMSO as a solvent, with the chemical shifts determined relative to the solvent peak. XRD were recorded on RIGAKU ULTIMA IV. The molar conductivity of the metal complexes in DMSO at 10^{-3} Molar concentration was measured using a dip cell and a Bibby conductivity meter MC1 at room temperature. The resistance measured in ohms and the molar conductivities were calculated according to the equation:

$$\Lambda_M = \frac{V \times K \times g}{Mw * \Omega}$$

where: Λ = molar conductivity (ohm^{-1} cm^2 mol^{-1}), V = volume of the complex solution, K = cell constant 0.92 cm^{-1}, Mw = molecular weight of the complex, g = weight of the complex, Ω = resistance measured in ohms. Electronic absorption spectra were recorded on UV-6100PCS double beam spectrometer using 1cm quartz cells taking DMSO as solvent. Magnetic susceptibilities were measured at 25°C by the Gouy method using mercuric tetrathiocyanatocobaltate(II) as the magnetic susceptibility standard. Diamagnetic corrections were estimated from Pascal's constant.[30] The magnetic moments were calculated from the equation:

$$\mu_{eff.} = 2.84\sqrt{\chi_M^{corr}.T}\ .$$

The thermal analyses (DTA and TGA) were carried out in air on a Shimadzu DT-30 thermal analyzer from 27 to 800 °C at a heating rate of 10 °C per minute.

2.3. Preparation of the ligand, 2-hydroxy-4-*p*-tolyldiazenyl) benzylidene)-2-(phenylamino) acetohydrazide (H_2L) (1)

2-hydroxy-5-(*p*-tolyldiazenyl) benzaldehyde (2.40 g, 0.01 mol, in 20 cm^3 of absolute ethanol) was added dropwise to 2-(phenylamino) acetohydrazide (1.65 g, 0.01 mol. in 20 cm^3 of absolute ethanol). The mixture was refluxed while stirring for one hour. The formed solid product was filtered off, washed with cold ethanol, followed by crystallization from ethanol and finally dried under vacuum over anhydrous $CaCl_2$. Yield: 84%, Color: yellow. *Elemental Anal.* Calcd. mass fractions of elements, w/%, C, 68.10; H, 5.50; N, 18.00. Found: C, 86.20; H, 5.41; N, 18.11. IR, (KBr, cm^{-1}): 3359(s) υ(OH), υ(NH^{11}) 3254, υ(NH^{7}) 3100, 1693 υ(C=O), 1606 υ(C=N), 1485 υ(N=N), 1260 $\upsilon(C\text{-}O)_{ph}$, 969 υ(N-N). ^{1}H-NMR (DMSO-d_6, 400 MHz): δ = 10.9 (s, 1H, O*H*), 11.85 (s, 1H, NH^{11}), 6.59 (s, 1H, NH^{7}), 8.59 (s, 1H, N=C-H^{13}), 6.61-8.38 ppm (m, 12 H, aromatic protons). ^{13}*C*-NMR (DMSO-d_6, 400 MHz): δ = 167.7 (C=O), 160.3 (C-OH), 150.6 (C-NH), 141.5 (C=NH), 112.9−130.4 (aromatic carbon), 40.52 (N-CH_2), 21.50 (CH_3),

2.4. Preparation of the metal complexes

Metal complexes, **(3), (5), (7)** and **(9-11)** were prepared by mixing a hot ethanoic solution of the following metal salts: $CuCl_2{\cdot}2H_2O$, $CuSO_4{\cdot}5H_2O$, $Co(CH_3COO)_2{\cdot}4H_2O$, $FeCl_3{\cdot}6H_2O$, $RuCl_3{\cdot}3H_2O$ and $VOSO_4{\cdot}H_2O$ respectively with a suitable amount of a hot ethanoic solution of the ligand in molar ratio 1M : 2 L (metal : ligand) in the presence of 2 cm^3 of triethylamine (TEA). The reaction mixture was then refluxed for 3 hours. The formed precipitates were filtered off, washed with ethanol, then with diethyl ether and dried under vacuum over anhydrous $CaCl_2$. The same method is used to prepare complexes; **(2)**, **(4), (6), (8)** and **(12)** but in 1M : 1L (metal : ligand) molar ratio using the following metal salts $Cu(CH_3COO)_2.H_2O$, $Cu(NO_3)_2.3H_2O$, $Ni(CH_3COO)_2.4H_2O$, $Mn(CH_3COO)_2.4H_2O$ and $Zn(CH_3COO)_2.2H_2O$

Complex **(2),** $[Cu(H_2L)(CH_3COO)_2]$, $C_{26}H_{27}CuN_5O_6$ (FW = 569.07),yield: 70%, melting points (M.P.) >300, color: dark brown, molar conductance (Λ) is 10.2 $\Omega^{-1}cm^2mol^{-1}$. *Elemental Anal.* calcd. mass fractions of elements, w/%, : C, 54.88; H, 4.78; N, 12.31; Cu, 11.17; found: C, 54.80.; H, 4.70; N, 12.41; Cu, 11.51; IR (KBr,

cm^{-1}): 3359 υ(OH), 3254 υ(NH1[11]), 3095 υ(CH_2NH^7), 1693 υ(C=O), 1606 υ(C=N), 1471 υ(N=N), 1260 υ(C-OH), 998 υ(N-N), 593 υ(M←O), 474 υ(M←N), 1531, 1372 (Δ=159) $\upsilon_{sym}CH_3COO$, $\upsilon_{asym}CH_3COO$.

Complex **(3),** $[Cu(H_2L)_2Cl_2].2H_2O$ $C_{44}H_{46}CuN_{10}O_6$ (FW = 945.32),yield: 62%, M.P.>300. Color: dark brown, molar conductance (Λ) is 13.1 $\Omega^{-1}cm^2mol^{-1}$. *Elemental Anal.* Calcd.: C, 55.90; H, 4.90; N, 14.82; Cu, 6.72; found: C, 55.81.; H, 5.01; N, 14.92; Cu, 6.04; IR (KBr, cm^{-1}): 3360 υ(OH), 3254 υ(NH1[11]), 3110 υ(CH_2NH^7), 1694υ(C=O), 1607 υ(C=N), 1466 υ(N=N), 1310 υ(C-OH), 1027 υ(N-N), 507 υ(M←O), 474 υ(M←N).

Complex **(4),** $[Cu(L)(H_2O)_3]$ $C_{22}H_{25}CuN_5O_5$ (FW = 503.01),yield: 75%, M.P.=270. Color: brown, molar conductance (Λ) is 7.8 $\Omega^{-1}cm^2mol^{-1}$. *Elemental Anal.* Calcd. mass fractions of elements, w/%, : C, 52.53; H, 5.01; N, 13.92; Cu, 12.63; found: C, 52.59.; H, 5.18; N, 13.61; Cu, 12.77; IR (KBr, cm^{-1}): 3120 υ(CH_2NH^7), 1607 υ(C=N), 1538 υ(*N=C*-O), 1465 υ(N=N), 1380 υ(*C*-O[10]), 1310 υ(C-O_{ph}), 1034 υ(N-N), 511 υ(M-O), 475 υ(M←N),

Complex **(5)**, $[Cu(H_2L)_2(SO_4)(H_2O].H_2O$, $C_{44}H_{46}CuN_{10}O_{10}S$ (FW = 970.51), yield: 71%, M.P.>300. Color: brown, molar conductance (Λ) is 28.5 $\Omega^{-1}cm^2mol^{-1}$. *Elemental Anal.* Calcd.: C, 54.45; H, 4.78; N, 14.43; Cu, 6.55; found: C, 54.49.; H, 4.88; N, 14.41; Cu, 6.69; IR (KBr, cm^{-1}): 3361υ(NH), 3255 υ(NH1[11]), 3088 υ(CH_2NH^7), 1693 υ(C=O), 1606 υ(C=N), 1467 υ(N=N), 1257 υ(C-OH), 1010 υ(N-N), 593 υ(M←O), 476 υ(M←N),

Complex **(6),** $[Ni(L)(H_2O)_3]$ $C_{22}H_{25}NiN_5O_5$ (FW = 498.16),yield: 70%, M.P.>300. Color: red, molar conductance (Λ) is 11.9 $\Omega^{-1}cm^2mol^{-1}$. *Elemental Anal.* Calcd.: C, 53.04; H, 5.06; N, 14.06; Ni, 11.78; found: C, 52.83.; H, 5.01; N, 14.16; Ni, 11.60; IR (KBr, cm^{-1}): 3150 υ(CH_2NH^7), 1603 υ(C=N), 1542 υ(*N=C*-O), 1467 υ(N=N), 1372 υ(*C*-O[10]), 1314 υ(C-O_{ph}), 1028 υ(N-N), 622, 595 υ(M-O), 513 υ(M←N).

Complex **(7),** $[Co(H_2L)_2(CH_3COO)_2]$, $C_{48}H_{48}CoN_{10}O_8$ (FW = 951.89),yield: 66%, M.P.>300. Color: brown, molar conductance (Λ) is 15.6 $\Omega^{-1}cm^2mol^{-1}$. *Elemental Anal.* Calcd.: C, 60.57; H, 5.08; N, 14.71; Co, 6.19; found: C, 60.50.; H, 5.17; N, 14.60; Co, 6.38; IR (KBr, cm^{-1}): 3360υ(OH), 3254 υ(NH1[11]), 3100 υ(CH_2NH^7), 1693 υ(C=O), 1603 υ(C=N), 1258 υ(C-OH), 1029 υ(N-N), 542 υ(M←O), 482 υ(M←N), 1537, 1371 (Δ= 166) $\upsilon_{sym}CH_3COO$, $\upsilon_{asym}CH_3COO$.

Complex **(8),** $[Mn(L)(H_2O)_3]$ $C_{22}H_{25}MnN_5O_5$ (FW = 494.40),yield: 77%, M.P.>300. Color: yellowish green, molar conductance (Λ) is 7.2 $\Omega^{-1}cm^2mol^{-1}$. *Elemental Anal.* Calcd.: C, 53.45; H, 5.11; N, 14.17; Mn, 11.11; Found: C, 53.15.; H, 5.41; N, 14.41; Mn, 11.00; IR (KBr, cm^{-1}): 3390 υ(OH), 3130 υ(CH_2NH^7),

1603 υ(C=N), 1544 υ(*N*=*C*-O), 1469 υ(N=N), 1378 υ(*C*-O[10]), 1298 υ(C-O_{ph}), 1023 υ(N-N), 631, 594 υ(M-O), 515 υ(M←N).

Complex **(9)**, $[Fe(H_2L)_2(Cl)_3]C_{44}H_{42}FeCl_3N_{10}O_4$ (FW = 937.07),yield: 58%, M.P.>300. Color: dark green, molar conductance (Λ) is 73.9 $\Omega^{-1}cm^2mol^{-1}$. *Elemental Anal.* Calcd.: C, 56.40; H, 4.52; N, 14.95; Fe, 5.96; Cl, 11.35; Found: C, 57.01.; H, 4.69; N, 15.30; Fe, 11.05; IR (KBr, cm^{-1}): 3360 υ(NH), 3255 υ(NH1[11]), 380 υ(CH_2NH^7), 1693 υ(C=O), 1604 υ(C=N), 1485 υ(N=N), 1258 υ(C-OH), 1011 υ(N-N), 564 υ(M←O), 469 υ(M←N).

Complex **(10), [**$Ru(H_2L)_2(Cl)_3$] $C_{44}H_{42}RuCl_3N_{10}O_4$ (FW = 982.30),yield: 77%, M.P.=277. Color: dark green, molar conductance (Λ) is 83.5 $\Omega^{-1}cm^2mol^{-1}$. *Elemental Anal.* Calcd.: C, 53.80; H, 4.31; N, 14.26; Ru, 10.29; found: C, 53.61.; H, 4.49; N, 14.51; Ru, 10.39; IR (KBr, cm^{-1}): 3360 υ(OH), 3255 υ(NH1[11]), 3100 υ(CH_2NH^7), 1693 υ(C=O), 1605 υ(C=N), 1485 υ(N=N), 1258 υ(C-OH), 1011 υ(N-N), 542 υ(M←O), 469 υ(M←N).

Complex **(11)**, $[VO(H_2L)_2(SO_4)]C_{44}H_{42}VN_{10}O_9S$ (FW = 937.87),Yield: 65%, M.P.=285. Color: yellowish green, molar conductance (Λ) is 23.4 $\Omega^{-1}cm^2mol^{-1}$. *Elemental Anal.* Calcd.: C, 56.35; H, 4.51; N, 14.93; V, 5.43; found: C, 56.32.; H, 4.61; N, 14.85; V, 5.51; IR (KBr, cm^{-1}): 3360 υ(OH), 3255 υ(NH1[11]), 3115 υ(CH_2NH^7), 1694 υ(C=O), 1605 υ(C=N), 1485 υ(N=N), 1271 υ(C-OH), 1033 υ(N-N), 564 υ(M←O), 468 υ(M←N).

Complex **(12), [**$Zn(H_2L)(CH_3COO)_2].2H_2O$, $C_{26}H_{31}ZnN_5O_8$ (FW = 606.93), yield: 60%, M.P.=270. Color: yellow, molar conductance (Λ) is 13.6.4 $\Omega^{-1}cm^2mol^{-1}$. *Elemental Anal.* Calcd.: C, 51.45; H, 5.15; N, 11.54; Zn, 10.77; found: C, 52.21.; H, 5.20; N, 11.11; Zn, 10.91; IR (KBr, cm^{-1}): 3180 υ(NH1[11]), 3090 υ(CH_2NH^7), 1706 υ(C=O), 1598 υ(C=N), 1451 υ(N=N), 1270 υ(C-OH), 1032 υ(N-N), 501 υ(M←O), 468 υ(M←N), 1544, 1356 (Δ= 180) $\upsilon_{sym}CH_3COO$, $\upsilon_{asym}CH_3COO$.

2.5. In-vitro antimicrobial activity

The antimicrobial activities of the ligand and its metal complexes were carried out in the Botany Department, Lab. of Microbiology, Faculty of Science, El-Menoufia University. They have been studied for their antimicrobial activities by the Well Diffusion Method[31]. The antibacterial and antifungal activities were evaluated against strands of *Escherichia coli* and *Aspergillus niger respectively*, at 250, 200 and 150 μg/mL concentrations in DMSO. A disc of poured DMSO was used as a negative control. The bacteria were subcultured in nutrient agar medium prepared using ($g.L^{-1}$ distilled water) NaCl (5 g), peptone (5 g), beef extract (3 g), agar (20 g). while

the fungus was subcultured in Czapek Dox´s medium prepared using ($g.L^{-1}$ distilled water) yeast extract (1g), sucrose (30 g), $NaNO_3$, agar (20 g), KCl (0.5 g), KH_2PO_4 (1 g), $MgSO_4.7H_2O$ (0.5 g) and trace of $FeCl_3.6H_2O$. This medium was then sterilized by autoclaving at 120 ºC for 15 min. After cooling to 45 ºC the medium was poured into 90 mm diameter Petri dishes and incubated at 28 ºC. After agar solidification, Petri dishes were stored at 4 ºC for few hours. Microorganisms were spread over each dish by using sterile bent Loop rod. Disks were cut by sterilized Cork borer and then taken by sterilized needle. The resulted pits are sites for the tested compounds of known concentration. Standard antibacterial (Tetracycline), and antifungal drugs (Amphotricene B) as well as solutions of metal salts were also screened under similar conditions for comparison. Plates were allowed to stand in a refrigerator for two hours before incubation to allow the tested compounds to diffuse through the agar. The Petri dishes were incubated for 48 h at 28. The growth inhibition zones around the holes were observed, indicating that the examined compound inhibits the growth of microorganism. The inhibition zone was measured in millimeters carefully. All determination was made in duplicate for each of the compounds. An average of the two independent readings for each compound was record.

3. Results and discussion

The reaction of 2-(phenylamino) acetohydrazide with 2-hydroxy-5-(p-tolyldiazenyl) benzaldehyde in EtOH in (1:1) molar ratio, led to the formation of the ligand H_2L^1 **(1)**, as shown in scheme 1. The reaction of the ligand **(1)** with metal salts using (2:1) mole ratios gives complexes; (**3), (5), (7)** and (**9-11),** while, changing the molar ratio to (1:1) gives complexes; **(2)**, **(4), (6), (8**) and **(12)** with different geometries. All the compounds are intensely colored, crystalline solids, and stable at room temperature and don't decompose after prolonged storage. The complexes are insoluble in water, ethanol, methanol, benzene, toluene, acetonitrile and chloroform, but completely soluble in dimethylformamide (DMF) or dimethylsulfoxide (DMSO). Elemental analyses, physical, spectral and XRD data are presented in Tables 1-4 and are compatible with the suggested structures shown in Figures 1-3. The elemental analyses confirmed that, the complexes (**3), (5), (7)** and (**9-11)** were composed in ML_2 formulae ratio, whereas complexes **(2)**, **(4), (6), (8**) and **(12)** were found to adopt the ML formula.

3.1. ^{1}H- and ^{13}C-NMR spectra of ligand

The ^{1}H- NMR spectrum of the ligand in DMSO-d^6 showed signals consistent with the proposed structure. The absence of the signal of the amino group ($-NH_2$) characteristic to the starting material (hydrazide) referring to their involvement in

the condensation reaction to form the ligand. The spectrum showed three sets of peaks, the first set observed as singlets at 10.9 (s, 1H), 11.85 (s, 1H), 6.59(s, 1H) ppm which may be assigned to the hydroxyl (OH^{20}), (NH^{11}) and (NH^{7}) protons respectively.[32-34] These hydrogen resonances appeared at higher δ values than expected, this could be assigned to their attachment to highly electronegative atoms, oxygen and nitrogen respectively. This assignment was confirmed by the remarkable intensity decreasing of these peaks in the deuterated spectrum of the ligand. The position of these signal in the downfield region indicates the possibility of their involvement in a considerable extent of hydrogen bonding. [33,34] The second set appeared as singlet at 8.59 (s, 1H) ppm was assigned to the azomethine proton of (H-C=N) group.[34, 35] The third resonance set observed as multiples in the 6.61–8.38 (m, 12H) ppm range was attributed to aromatic protons. It was clear from the ^{1}H-NMR spectrum of the ligand that it exhibits the keto-form only and no evidence for the presence of the enol-form. This result was supported by the presence of the signals related to the (NH) and phenolic (OH) only and the absence of the (OH) signal of the enol-form. The same conclusion was reported by many authors.[33, 34] The ^{13}C-NMR spectrum showed different peaks appearing at 167.7 and 160.3 ppm. These peaks can be due to C=O and –C-OH groups respectively[35, 36] The peaks at 150.6 and 141.5 ppm can be due to C-NH and CH=N- groups respectively.[35] However the peaks at 112.9-130.4 ppm range are assigned to the carbons of aromatic ring.[36] The peaks appearing at 40.52 and 21.5 ppm may be due to $–CH_2$-N and CH_3 groups respectively.[37]

3.2. Conductivity Measurements

The molar conductivity of 1×10^{-3}M solutions of the metal complexes in DMSO at room temperature for all compounds except complexes **(9)** and **(10)** are in the 6.4–23.5 $\Omega^{-1}cm^2mol^{-1}$ range (experimental part) indicating to the non-electrolytic nature of these compounds[38], and supporting the proposed structures having the anions coordinated to metal ions. The considerably high values of some complexes may be due to the partial solvolysis by DMSO. The molar conductivity of complexes **(9)** and **(10)** are 73.9 and 84.5 $\Omega^{-1}cm^2mol^{-1}$ respectively indicating the electrolytic nature of these complexes. These data are agreeable with Greenwood et al. studies.[39]

3.3. IR Spectra

The bonding mode of the ligand in the metal complexes has been deduced from their IR spectra. Important spectral bands of the ligand and its metal complexes are presented in the experimental part. The spectrum of the ligand (H_2L) showed a

strong band at 3254 cm^{-1}, which may be assigned to υ(NH^{11}) group, whereas the strong band at 1693 cm^{-1} may be due to the carbonyl group of the hydrazide moiety[32, 33]. This observation indicated that, the ligand presents in the ketonic form in the solid state[40]. The spectrum showed a sharp band at 3359 cm^{-1} which may be assigned to the stretching vibration of the phenolic hydroxyl group [31]. The relatively strong and medium bands located at 3100, 1606, 1485 and 969 cm^{-1} corresponded to the amine group (CH_2-NH^7), azomethine group[41], azo group[42], and υ(N-N) linkage[31] respectively. The band appeared at 1260 cm^{-1} is due to the υ(C-OH) of the phenolic moiety[40]. The mode the ligand-metal bonding can be predicted by comparison the IR spectra of the complexes with that of the free ligand. The IR spectral data showed that, the ligand behaves as either of the following: 1) Neutral bidentate as in case of complexes **(2), (3), (5), (7),** and **(9-12)** in which the ligand coordinated to metal ions via ketonic carbonyl oxygen and azomethine nitrogen atoms. This mode of coordination was supported by the following evidences: i) the band characteristic to υ(NH^{11}) is still present and the carbonyl group is appeared as a medium intensity band indicating that, in these complexes, the ligand coordinated to metal ion via ketonic carbonyl oxygen; ii) the band characteristic to azomethine group υ(C=N) appeared as week band. At the same time, the band due to υ(N-N) was shifted to a higher frequency and appearing in the 998-1033 cm^{-1} range. The increasing in the frequency of this band υ(N-N) is a clear indication to the increasing in the double bond character is off-setting the loss of electron density via electron donation to the metal ions and further confirmation of the coordination of the ligand via the azomethine group[41]. 2) Dibasic tridentate bonding through the enolic carbonyl oxygen (C-O), deprotonated hydroxyl oxygen and azomethine nitrogen (C=N) atoms as in complexes **(4), (6)** and **(8)**. This mode of bonding was suggested by the following evidences: i) the bands characteristic to the carbonyl υ(C=O), and υ(NH) groups disappeared indicating that, the ligand bonded to the metal ions in its enol-form via enolic carbonyl oxygen atom, which is further supported by the appearance of new bands in the 1538–1544 and 1372–1380 cm^{-1} ranges corresponding to the υ(N=C-O), and υ(C-O), respectively[43] ii) the band characteristic to azomethine group υ(C=N) shifted or appeared as week band in the 1603-1607 cm^{-1} range. At the same time, the band due to υ(N-N) was shifted to a higher frequency and appearing in the 1023-1034 cm^{-1} range. The increasing in the frequency of this band υ(N-N) is a clear indication to the increasing in the double bond character is off-setting the loss of electron density via electron donation to the metal ions and further confirmation of the coordination of the ligand via the azomethine group[41]. iii) The shifting in the band characteristic to phenolic oxygen atom and disappearing of the band assigned to the hydroxyl proton indicating that, the bonding occurs via the deprotonated phenolic oxygen atom. The appearance of new bands in the 504–631 and 468–515 cm^{-1} ranges for all complexes may be assigned to the υ(M—O), υ(M←O) and υ(M←N) respectively[44]. The appearance of these bands was taken as a confirmation for the ligand-metal ions bonding via the

carbonyl oxygen atom (enolic or ketonic), azomethine nitrogen atom and/or deprotonated phenolic hydroxyl oxygen atom. The IR spectrum of the sulfate complexes **(5)** and **(11)** revealed the presence of new bands at 1257, 1193, 1158, 869 and 1271, 1201, 1157, 893 cm^{-1} for the two complexes respectively. These bands indicate that the sulphate ion is coordinated to the copper(II) and vanadyl(II)) ion in a uni-dentate chelating fashion[45, 46]. In the case of acetate complexes **(2), (7)** and **(12)** two new bands appeared in the 1531-1544 and 1356-1372 cm^{-1} ranges, which are attributed to the symmetric and asymmetric stretching vibration of the acetate group. The mode of coordination of acetate group has often been deduced from the magnitude of the observed separation between the $\upsilon_{asy.}(COO)$ and $\upsilon_{sy.}(COO)$. In acetate complexes, the acetate ion may coordinate to the metal ion in a uni-dentate, a bi-dentate or a bridging bi-dentate manner. The $\upsilon_{as}(CO_2)$ and $\upsilon_{s}(CO_2)$ of the free acetate ion are ca. 1560 and 1416 cm^{-1} respectively. In unidentate acetate complexes, $\upsilon(C=O)$ is higher than $\upsilon_{s}(CO_2)$ and $\upsilon(C\text{-}O)$ is lower than $\upsilon_{as}(CO^{2-})$. As a result the separation between the two $\upsilon(CO)$ is much larger in uni-dentate than in free ion on the other hand, in the bidentate fashion, the separation is lower than in the free ion while in the bridging bidentate the two $\upsilon(CO)$ is closer to the free ion[47]. The separation values (Δ) between $\upsilon_{asym}(COO)$ and $\upsilon_{sym.}(COO)$ in our acetate complexes were in the 159-180 cm^{-1} range suggesting the coordination of acetate group in a mono-dentate fashion[45, 46, 48]. The infrared spectra of the vanadyl(II) complex **(11)** revealed a medium band at 969 cm^{-1} which may be attributed to $\upsilon(V=O)$[47]. The broad bands in the 3405–3360 cm^{-1} region are due to coordinated water or water of crystallization. The bands for water of crystallization are different from those of coordinated water; the latter has bands in the 970–930 and 657–623 cm^{-1} regions. The absence of these signals in the spectra of the complexes **(3)**, **(11)** and **(12)** indicated to no presence for coordinated water molecules. The presence of water molecules within the coordination sphere in the complexes **(4)**, **(5), (6)** and **(8)** were supported by the presence of bands in the 3407–3390, 1570–1579, 940–945 and 635–650 cm^{-1} due to OH stretching, HOH deformation, H_2O rocking and H_2O wagging, respectively[49].

3.4. Magnetic Moment

The magnetic moments of the complexes **(2–11)** at room temperature were collected in Table 1. The results showed that, all complexes are paramagnetic. The copper(II) complexes **(2–5)** recorded values in the 1.72–1.80 BM range which are consistent with presence of one unpaired electron system in an octahedral environment.[33] Nickel(II) complex **(6)** shows 2.95 BM value which is consistent with two unpaired electrons system of octahedral nickel(II) complex.[42] Cobalt(II) complex **(7)** recorded 4.12 BM value, corresponding to a high spin cobalt(II) complex.[50] The magnetic moment values of manganese(II) **(8)** and iron(III)

complexes **(9)** are 5.67 and 5.90 BM respectively which is an indicative for five unpaired electrons of an octahedral system. The magnetic moment value of ruthenium(III) complex **(10)** is 1.68 BM which is a characteristic for d^5 low spin ruthenium$^{(III)}$ complex[50] vanadyl(II) complex **(11)** shows a magnetic value equal to 1.75 BM which is corresponding to one unpaired electron.[43, 46]

3.5. Electronic absorption Spectra

The electronic absorption spectral data of the ligand and its metal complexes in DMF solutions are summarized in Table 1**.** The structure of the ligand revealed that, the two lone electron pairs of azo group are not the only interacting non-bonding electrons, since the hydrazone moiety of the ligand contains nitrogen and oxygen atoms representing extra sources of lone pair of electrons. Thus other $n\rightarrow\pi^*$ transitions is expected to take place from these non-bonding orbitals to different molecular orbital extending over such large molecules.[51] The data revealed that, the ligand comprised three sets of peaks in the UV and visible regions. The first set of the shortest wavelengths appeared at 225 and 245 nm may be assigned to the $\pi\rightarrow\pi^*$ transitions in the intra ligand and benzenoid moiety.[35,49] The second set observed at 320 and 335 nm may be assigned to $n\rightarrow\pi^*$ transitions of the azomethine and carbonyl groups.[35,49] The third set comprise of two bands: the first one located at 370 nm, which could be attributed to $\pi\rightarrow\pi^*$ transition involving the π electron of the azo group.[51, 52] Whereas the second band located in the visible region at 395 nm could be assigned to $\pi\rightarrow\pi^*$ transition involving the whole electronic system of the compounds with a considerable charge transfer character arising mainly from the phenolic moiety. [51, 52] Complex **(2)** showed peaks at 410, 480 and 590 nm, corresponding to $^2B_{1g}\rightarrow{}^2B_{2g}$, $^2B_{1g}\rightarrow{}^2E_g$ and $^2B_{1g}\rightarrow{}^2A_{1g}$ transitions respectively characteristic to a square planar copper(II) complex [Fig. 1][53, 54].[53, 54] The electronic spectrum of copper(II) complexes **(3), (4)** and **(5)** in DMF solution showed a broad band centered in the 600–635 nm range. The position as well as the broadness of this band indicated that copper(II) has a tetragonally distorted octahedral geometry [Figs. 1,2]. This broad band consists of three superimposed transitions $^2B_{1g}\rightarrow{}^2E_g$, $^2B_{1g}\rightarrow{}^2A_{1g}$ and $^2B_{1g}\rightarrow{}^2B_{2g}$ [48, 55][48, 55] Nickel(II) complex **(6)** exhibits three bands located at 530, 580, 790 nm which may be assigned to $^3A_{2g}(F)\rightarrow{}^3T_{1g}(P)(\upsilon_3)$, $^3A_{2g}(F)\rightarrow{}^3T_{1g}(F)(\upsilon_2)$ and $^3A_{2g}(F)\rightarrow{}^3T_{2g}(F)(\upsilon_1)$ spin allowed transitions, which are characteristic to nickel(II) ion in an octahedral structure [Figs. 1,2].[52,(56, 57)] The υ_2 / υ_1 ratio for the complex is 1.36 which is less than the usual range (1.5-1.75), indicating a distorted octahedral nickel(II) complex.[58] The cobalt(II) complex **(7)** showed bands at 440, 550, 570 nm, which ware assigned to $^4T_{1g}(F)\rightarrow{}^4T_{1g}(P)$**,** $^4T_{1g}(F)\rightarrow{}^4A_{2g}$ and $^4T_{1g}(F)\rightarrow{}^4T_{2g}(F)$, transitions respectively, corresponding to high spin cobalt(II) octahedral complex [Figs. 1,2][55, 59] Manganese(II) complexes **(8)**

displays week absorption bands at 460, 500, 570 and 670 nm assigned to $^6A_{1g}\rightarrow{}^4T_{1g}(4G)(\upsilon_1)$, $^6A_{1g}\rightarrow{}^4E_g(4G)(\upsilon_2)$, $^6A_{1g}\rightarrow{}^4E_g(4D)(\upsilon_3)$ and $^6A_{1g}\rightarrow{}^4T_{1g}(4p)(\upsilon_4)$ transitions respectively, which characteristic to manganese(II) in an octahedral geometry.[53, 57] Iron(III) complex **(9)** gave bands at 560 and 670 nm which may be assigned to $^6A_{1g}\rightarrow{}^4T_{2g}$ and $^6A_{1g}\rightarrow{}^4T_1(G)$ transitions. These bands are characteristic of an octahedral iron(III) complex[53, 56, 57, 60] However the electronic absorption spectrum of ruthenium(III) complex **(10)** displayed two bands at 530 and 650 nm. The first band may be due to LMCT transition and the second may be assigned to $^2T_{2g}\rightarrow{}^2A_{2g}$ transition. The band positions are similar to those observed for other octahedral ruthenium(III) complex [52, 53] The electronic spectrum of vanadyl(II) complex **(11)** showed that, there are three bands at 515, 600, 720 nm which may be assigned to $^2B_2(d_{xy})\rightarrow{}^2E(d_{xz},d_{yz})$, $^2B_2(dxy)\rightarrow{}^2B_1(d_{x2-y2})$ and $^2B_2(dxy)\rightarrow A_1(d_{z2})$ transitions respectively indicating that, the vanadyl(II) complex has a distorted octahedral structure (Fig. 3).[52, 55] The bands observed in the diamagnetic zinc(II) complex **(12)** are due to intraligand transitions.

3.6. X-ray powder diffraction analysis

X-ray powder diffraction analysis of complexes **(3)** and **(4)** were carried out to determine the type of crystal system, lattice parameters, and the cell volume. The XRD patterns indicate to the crystalline nature of the two complexes. Indexing of the diffraction patterns was performed using Ultima IV multipurpose diffraction system Plus Chekcell software. Miller indices (*hkl*) along with observed and calculated 2θ angles, *d* values, and relative intensities are given in Tables (2, 3) for complexes (**3**) and (**4**). From the indexed data the unit cell parameters were also calculated and are listed in Table (4). The powder XRD patterns of the compounds are completely different from those of the starting materials, demonstrating the formation of coordination compounds. It is found that the samples have monoclinic structures. The crystal structures of similar type of samples were reported as monoclinic and orthorhombic.[61, 62] The mean crystallite sizes of the complexes, *D*, were also determined according to the Scherrer equation ($D = 0.9\lambda/(\beta\cos\theta)$, where λ is X-ray wavelength (1.5406 A), θ is Bragg diffraction angle, and β is the full width at half maximum of the diffraction peak). The average crystallite sizes of all the samples were found to be around *54.83* nm and the values are given in Table (4).

3.7. Thermal Analyses (TGA)

Since the IR spectra indicate the presence of water molecules, thermal analyses (TGA) was carried out to ascertain their nature. Complex **(3)** decomposed in three steps. The first step occurred at 65 °C with 3.5% weight loss (calcd 3.8%)

corresponding well to elimination of two hydrated water molecules. The second step occurred at 220-350 ^{o}C range with 7.6% weight loss (calcd 7.8%) due to elimination of two HCl molecules. The third step occurred at 400-580 ^{o}C with 78.9% weight loss (calcd 80.27%), refers to the complete decomposition of the complexes, which ended up with the formation of CuO. Complex **(5)** decomposed in four steps. The first step occurred at 75 ^{o}C with 2.01% weight loss (calcd 1.85 %) due to elimination of one hydrated water molecule. The second step occurred at 120-200 ^{o}C range with 1.91 % weight loss (calcd 1.85%) due to elimination of one coordinated water molecule. The third step occurred in the 300-340 ^{o}C range with 10.12% weight loss (calcd 9.89%) due to elimination of a sulphate group (H_2SO_4). The fourth step occurred at 400-580 ^{o}C with 73.99% weight loss (calcd 74.50%), refers to the complete decomposition of the complexes, which ended up with the formation of CuO. Complexes **(4)**, **(6)** and **(8)** decomposed in tow steps. The first step occurred at 120-200 ^{o}C range with 10.81%, 10.71% and 10.69% weight loss (calcd 10.74%, 10.84% and 10.92%) due to elimination of coordinated water molecules ($3H_2O$). The second step occurred at 400-580 ^{o}C with 72.91%, 72.87% and 74.01% weight losses (calcd 73.50%, 74.15% and 74.79%), corresponding to the complete decomposition of the complexes which ended up with the formation of CuO, NiO and MnO respectively. Complexes **(9)** and **(10)** decomposed in two steps. The first step occurred at 240-360^{0}C range with 10.35%, 10.83% weight losses (calcd 11.35%, 10.83%) respectively due to elimination of two HCl molecules. The second step occurred at 400-580 ^{o}C with 78.93%, 75.03% weight losses (calcd 80.14%, 76.44%) respectively, corresponding to the complete decomposition of the complexes which ended with the formation of Fe_2O_3, Ru_2O_3 respectively. Complex **(12)** decomposed in three steps. The first step occurred at 85 ^{o}C with 6.45% weight loss (calcd 6.58%) due to elimination of two hydrated water molecules, whereas the second step took place in the 180-250 ^{o}C range with 20.96% weight loss (calcd 21.57%) due to elimination of ($2CH_3COOH$). The third step occurred at 370-540 ^{o}C with 74.69% weight loss (calcd 75.02%), refers to the complete decomposition of the complexes which ended up with the formation of ZnO.

3.8. Antibacterial and Antifungal Screening

The ligand and its metal complexes have been screened for their antibacterial and antifungal activities at different concentration using well diffusion method against *E. Coli and Aspergillus Niger* and the obtained results are presented in Table 5. It is observed that, the antimicrobial activities of the compounds enhanced upon increasing the concentration, and the metal complexes are showing more potent activities than the parent ligand**.** Chelation theory could utilized to describe this improvement in the activity.[63, 64] Upon chelation, the partial sharing of the metal

ions positive charge with the donor groups accompanied with the possible π-electron delocalization on the whole chelate ring resulted in reducing the polarity of the metal ion considerably, mainly because of the lipid and polysaccharides are some important constituents of cell walls and membranes, which are preferred for metal ion interaction. In addition to this, the cell wall also contains many amino phosphates, carbonyl and cysteinyl ligands, which maintain the integrity of the membrane by acting as diffusion barrier and also provides suitable sites for binding. Chelation can reduce not only the polarity of the metal ion, but also increases the lipophilic character of the chelate and the interaction between metal ions and the lipid is favored. This may lead to the breakdown of the permeability barrier of the cell resulting in interference with the normal cell processes. If the geometry and charge distribution around the molecule are incompatible with geometry and charge distribution around the pores of the bacterial cell wall, penetration through the wall by the toxic agent cannot take place and this will prevent the toxic reaction within the pores. Chelation is not the only criterion for the antibacterial activity. Some important factors such as the nature of the metal ion, nature of the ligand, coordinating sites, and geometry of the complex, concentration, hydrophobicity, lipophilicity and presence of co-ligands have considerable influence on antibacterial activity. Certainly, steric and pharmacokinetic factors also play a decisive role in deciding the potency of an antimicrobial agent. The results show that, complex **(11)** exhibits the highest antifungal activity, in the time that complex **(4)** exhibits the highest antibacterial among the tested compounds. The order of antifungal activity for the compounds is: **(11)** > **(4)** = **(10)** > **(9)** > **(3)** = **(12)** > **(ligand)** > **(5)** = **(7)** = **(8)** > **(6).** While the order of antibacterial activity is: **(4)** > **(Ligand)** > **(7)** > **(2)** = **(3)** = **(11)** > **(10)** > **(9)** > **(6)** > **(5)** > **(12)**.

4. Conclusion

Mononuclear $Zn^{(II)}$, $Cu^{(II)}$, $Ni^{(II)}$, $Co^{(II)}$, $Mn^{(II)}$, $Fe^{(III)}$, $Ru^{(III)}$ and $V^{(IV)}O$ complexes of with a novel azohydraozne acetohydrazide ligand were synthesized. The ligand as well as the metal complexes were characterized by spectral (^{1}H, ^{13}C-NMR, IR, U.V, XRD), elemental and thermal analyses, magnetic moment and molar conductance measurements. . The elemental analyses data referred that, the complexes (**3), (5), (7)** and (**9-11)** were composed in 1:2 (metal : ligand) stoichiometry whereas complexes **(2)**, **(4), (6), (8**) and **(12)** were found to adopt (1:1) stoichiometry. The molar conductivity measurements indicate to a non-electrolytic nature of all complexes except complexes **(9)** and **(10)** which recorded 73.9 and 84.5 $\Omega^{-1}cm^{2}mol^{-1}$ values respectively indicating their electrolytic nature. The IR spectral data suggest that the ligand behaves as neutral bidentate or a dibasic tridentate moiety with *ONO* donor atoms. XRD patterns indicated the copper complexes (**3, 4**) possess a monoclinic structures with average crystallite sizes

around *54.83 nm*. The antibacterial and antifungal activities of the ligand and its metal complexes were evaluated against bacterial species: *Escherichia coli* and *Aspergillus niger*. The activity data showed that the metal complexes have a promising biological activity comparable with the parent ligand and they are more fungicides than bactericides.

5. References

[1] Patil M, Hunoor R & Gudasi K, *European Journal of Medicinal Chemistry*, *45* (2010) 2981.

[2] Refat H M & Fadda A, *European Journal of Medicinal Chemistry*, *70* (2013) 419.

[3] Altıntop M D, Kaplancıklı Z A, Çiftçi G A & Demirel R, *European Journal of Medicinal Chemistry*, *74* (2014) 264.

[4] Yousef T, El-Reash G A, El-Gammal O & Bedier R, *Journal of Molecular Structure*, *1029* (2012) 149.

[5] Ebrahimipour S Y, Sheikhshoaie I, Crochet A, Khaleghi M & Fromm K M, *Journal of Molecular Structure*, *1072* (2014) 267.

[6] Altıntop M D, Özdemir A, Turan-Zitouni G, Ilgın S, Atlı Ö, İşcan G & Kaplancıklı Z A, *European Journal of Medicinal Chemistry*, *58* (2012) 299.

[7] Wardakhan W W, EL-SAYED N N & Mohareb R M, *Acta pharmaceutica*, *63* (2013) 45.

[8] El-Tabla A S, Abdelwahed M M, Whaba M A & Abouelfadl N A, *Bioinorganic Chemistry and Applications Volume 2015:*, *2015* (2015) 1.

[9] El-Tabla A S, Abdelwahed M M, Whaba M A & Shebl M A, *Journal of Advances in Chemistry*, *11* (2015) 3888.

[10] Badiger D S, Hunoor R S, Patil B R, Vadavi R S, Mangannavar C V, Muchchandi I S, Patil Y P, Nethaji M & Gudasi K B, *Inorganica chimica acta*, *384* (2012) 197.

[11] Netalkar P P, Netalkar S P, Budagumpi S & Revankar V K, *European Journal of Medicinal Chemistry*, *79* (2014) 47.

[12] Gökçe M, Utku S & Küpeli E, *European Journal of Medicinal Chemistry*, *44* (2009) 3760.

[13] Kaushik D, Khan S A, Chawla G & Kumar S, *European Journal of Medicinal Chemistry*, *45* (2010) 3943.

[14] Khan K M, Rasheed M, Ullah Z, Hayat S, Kaukab F, Choudhary M I & Perveen S, *Bioorganic & Medicinal Chemistry*, *11* (2003) 1381.

[15] Sangshetti J N, Shaikh R I, Khan F A K, Patil R H, Marathe S D, Gade W N & Shinde D B, *Bioorganic & Medicinal Chemistry Letters*, *24* (2014) 1605.

[16] Özer E Ö, Tan O U, Ozadali K, Küçükkılınç T, Balkan A & Uçar G, *Bioorganic & Medicinal Chemistry Letters*, *23* (2013) 440.

[17] Shabbir A, Shahzad M, Ali A & Zia-ur-Rehman M, *European Journal of Pharmacology*, *738* (2014) 263.

[18] Datta A, Liu P-H, Huang J-H, Garribba E, Turnbull M, Machura B, Hsu C-L, Chang W-T & Pevec A, *Polyhedron*, *44* (2012) 77.

[19] El-Gammal O A, Elmorsy E A & Sherif Y E, *Spectrochimica Acta Part A: Molecular and Biomolecular Spectroscopy*, *120* (2014) 332.

[20] Hayat F, Salahuddin A, Umar S & Azam A, *European Journal of Medicinal Chemistry*, *45* (2010) 4669.

[21] Guzar S H & JIN Q-h, *Chemical Research in Chinese Universities*, *24* (2008) 143.

[22] Revanasiddappa H & Manju B, *European Journal of Pharmaceutical Sciences*, *9* (1999) 221.

[23] Bagherzadeh M, Zare M, Amani V, Ellern A & Woo L K, *Polyhedron*, *53* (2013) 223.

[24] El Meligy M G, El Rafie S & Abu-Zied K M, *Desalination*, *173* (2005) 33.

[25] Liu J-N, Wu B-W, Zhang B & Liu Y, *Turkish Journal of Chemistry*, *30* (2006) 41.

[26] Emam S, AbouEl-Enein S, El-Saied F & Alshater S, *Spectrochimica Acta Part A: Molecular and Biomolecular Spectroscopy*, *92* (2012) 96.

[27] Svehla G, *Vogel's Textbook of macro and semimicro qualitative inorganic analysis*, (Longman London, 1979;

[28] Welcher F J, *Am. Chem. Soc.*, *80* (1958) 2600.

[29] Vogel A, *A Text Book of Quantitative Inorganic Analysis*, (ELBS, London) 1978; 474.

[30] B. Figgis, J. Lewis & Wilkins R, *Modern coordination chemistry*, (Interscience, New York) 1960;

[31] Collee J, (1989)

[32] Maurya M R, Khurana S, Schulzke C & Rehder D, *European Journal of Inorganic Chemistry*, *2001* (2001) 779.

[33] Gup R & Kırkan B, *Spectrochimica Acta Part A: Molecular and Biomolecular Spectroscopy*, *62* (2005) 1188.

[34] Raj B B, Kurup M P & Suresh E, *Spectrochimica Acta Part A: Molecular and Biomolecular Spectroscopy*, *71* (2008) 1253.

[35] Bayoumi H A, Alaghaz A-N M & Aljahdali M S, *Int. J. Electrochem. Sci*, *8* (2013) 9399.

[36] Kurtoğlu M, İspir E, Kurtoğlu N & Serin S, *Dyes and Pigments*, *77* (2008) 75.

[37] Han H O, Kim S H, Kim K-H, Hur G-C, Yim H J, Chung H-K, Woo S H, Koo K D, Lee C-S & Koh J S, *Bioorganic & Medicinal Chemistry Letters*, *17* (2007) 937.

[38] Geary W J, *Coordination Chemistry Reviews*, *7* (1971) 81.

[39] Greenwood N, Straughan B & Wilson A E, *Journal of the Chemical Society A: Inorganic, Physical, Theoretical*, (1968) 2209.

[40] Xu G-C, Zhang L, Liu L, Liu G-F & Jia D-Z, *Polyhedron*, *27* (2008) 12.

[41] Samanta B, Chakraborty J, Shit S, Batten S R, Jensen P, Masuda J D & Mitra S, *Inorganica chimica acta*, *360* (2007) 2471.

[42] Bhosale J D, Shirolkar A R, Pete U D, Zade C M, Mahajan D P, Hadole C D, Pawar S D, Patil U D, Dabur R & Bendre R, *Journal of Pharmacy Research*, *7* (2013) 582.

[43] Singh B & Srivastava P, *Transition Metal Chemistry*, *12* (1987) 475.

[44] El-Wahab Z A, Mashaly M M, Salman A, El-Shetary B & Faheim A, *Spectrochimica Acta Part A: Molecular and Biomolecular Spectroscopy*, *60* (2004) 2861.

[45] Nakamoto K, *Infrared and Raman spectra of inorganic and coordination compounds*, (Wiley Online Library, 1986;

[46] Chandra S & Gupta L K, *Spectrochimica Acta Part A: Molecular and Biomolecular Spectroscopy*, *61* (2005) 1181.

[47] El-Dissouky A, Fahmy A & Amer A, *Inorganica chimica acta*, *133* (1987) 311.

[48] El-Tabl A S, Shakdofa M M & Shakdofa A M, *Journal of the Serbian Chemical Society*, *78* (2013) 39.

[49] Remya P, Suresh C & Reddy M, *Polyhedron*, *26* (2007) 5016.

[50] Fouda M F, Abd-Elzaher M M, Shakdofa M M, El-Saied F A, Ayad M I & El Tabl A S, *Journal of Coordination Chemistry*, *61* (2008) 1983.

[51] Rageh N, Abdel Mawgoud A & Mostafa H, *Chemical Papers-Slovak Academy Of Sciences*, *53* (1999) 107.

[52] Gup R, Giziroglu E & Kırkan B, *Dyes and Pigments*, *73* (2007) 40.

[53] Lever & Philip A B, *Inorganic electronic spectroscopy*, (Elsevier, Amsterdam) 1968;

[54] Al-Hakimi A N, El-Tabl A S & Shakdofa M M, *Journal of Chemical Research*, *2009* (2009) 770.

[55] El-Tabl A S, Aly F A, Shakdofa M M & Shakdofa A M, *Journal of Coordination Chemistry*, *63* (2010) 700.

[56] Graham B, Spiccia L, Skelton B W, White A H & Hockless D C, *Inorganica chimica acta*, *358* (2005) 3974.

[57] Krishnapriya K & Kandaswamy M, *Polyhedron*, *24* (2005) 113.

[58] El-Tabl A S & El-Enein S A, *Journal of Coordination Chemistry*, *57* (2004) 281.

[59] Bedia K-K, Elçin O, Seda U, Fatma K, Sevim R & Dimoglo A, *European Journal of Medicinal Chemistry*, *41* (2006) 1253.

[60] Parihari R, Patel R & Patel R, *JOURNAL OF THE INDIAN CHEMICAL SOCIETY*, *77* (2000) 339.

[61] Wang C-C, *Zeitschrift für Kristallographie-New Crystal Structures*, *221* (2006) 385.

[62] Moubaraki B, Murray K S & Tiekink E R T, *Zeitschrift für Kristallographie-New Crystal Structures*, *217* (2002) 219.

[63] T.J. Franklin & G.A. Snow Eds., Chapman and Hall: London (1971); Vol.

[64] Collins C & Lyne P, *University Park Press, Baltimore, USA*, *234* (1970) 235.

List of tables

Table 1:- UV-Vis. spectra of the ligand (H_2L) and its metal complexes.

No	Bands in DMF	Electronic transition	μ_{eff} (BM)	Geometry
1	225, 245, 325, 340, 370 395			
2	230, 250, 330, 360, 390, 410, 480, 590	$^2B_{1g}\rightarrow{}^2B_{2g}$, $^2B_{1g}\rightarrow{}^2E_g$, $^2B_{1g}\rightarrow{}^2A_{1g}$	1.80	square planar
3	230, 255, 295, 335, 393, 600	$^2B_{1g}\rightarrow 2E_g$, $^2B_{1g}\rightarrow{}^2A_{1g}$,$^2B_{1g}\rightarrow{}^2B_{2g}$	1.72	tetragonal distorted octahedral
4	250 , 260, 295, 330, 393, 620		1.77	
5	240, 280, 335, 365, 394, 635		1.67	
6	240, 270, 350 , 370, 395, 530, 580, 790	$^3A_{2g}(F)\rightarrow{}^3T_{1g}(P)(\upsilon_3)$, $^3A_{2g}(F)\rightarrow{}^3T_{1g}(F)(\upsilon_2)$ $^3A_{2g}(F)\rightarrow{}^3T_{2g}(F)(\upsilon_1)$	2.95	octahedral
7	230, 260, 300, 370, 400, 440, 550, 570	$^4T_{1g}(F)\rightarrow{}^4T_{1g}(P)$, $^4T_{1g}(F)\rightarrow{}^4A_{2g}$ and $^4T_{1g}(F)\rightarrow{}^4T_{2g}(F)$,	4.12	octahedral
8	235, 260, 305,380 ,460, 500, 570, 670	$^6A_{1g}\rightarrow{}^4T_{1g}(4G)(\upsilon_1)$, $^6A_{1g}\rightarrow{}^4E_g(4G)(\upsilon_2)$, $^6A_{1g}\rightarrow{}^4E_g(4D)(\upsilon_3)$ and $^6A_{1g}\rightarrow{}^4T_{1g}(4p)(\upsilon_4)$,	5.67	octahedral
9	250, 320, 350, 390, 410, 560, 670	$^6A_{1g}\rightarrow{}^4T_{2g}$ and$^6A_{1g}\rightarrow{}^4T_1(G)$	5.90	octahedral
10	250, 310, 340, 370, 410, 530, 650	$^2T_{2g}\rightarrow{}^2A_{2g}$	1.68	octahedral
11	245, 280, 310, 348, 375, 515, 600, 720	$^2B_2(d_{xy})\rightarrow{}^2E(d_{xz},d_{yz})$, $^2B_2(dxy)\rightarrow{}^2B_1(d_{x2-y2})$ $^2B_2(dxy)\rightarrow A_1(d_{z2})$	1.75	distorted octahedral
12	220, 270, 305, 330, 347, 390		Dia.	

Table 2: Miller indices (*hkl*), observed, calculated 2θ angles, *d* values, and relative intensities for complex (3)

Peak No.	H	K	L	2Th(Found)	2Th(Calcd)	d-sp. A	Rel. Int.
1	-2	1	0	17.58	17.53	5.0407	7
2	-2	1	3	19.21	19.234	4.6165	6
3	0	1	4	24.12	24.125	3.6867	6
4	2	1	2	24.46	24.5	3.6362	8
5	-2	3	1	25.88	25.879	3.4398	8
6	-2	2	4	26.07	26.057	3.4152	8
7	1	2	3	26.2	26.19	3.3985	8

Peak No.	H	K	L	2Th(Found)	2Th(Calcd)	d-sp. A	Rel. Int.
8	-3	2	1	26.49	26.493	3.362	8
9	1	1	4	28.46	28.444	3.1336	5
10	-1	5	2	37.58	37.576	2.3914	100
11	3	2	3	38.36	38.359	2.3446	5
12	0	6	1	43.78	43.784	2.0661	38
13	6	4	2	64.02	64.023	1.4532	12
14	-4	7	6	64.19	64.19	1.4497	9
15	1	9	5	77.19	77.191	1.2348	37
16	-2	4	13	81.31	81.31	1.1823	23

Table 3: Miller indices (*hkl*), observed, calculated 2θ angles, *d* values, and relative intensities for complex (4)

Peak No.	H	K	L	2Th(Found)	2Th(Calcd)	d-sp. A	Rel. Int.
1	1	1	1	12.93	13.035	6.8411	12
2	-2	3	1	25.71	25.827	3.4622	10
3	-2	3	1	25.74	25.827	3.4582	11
4	-3	1	4	26.84	26.836	3.3189	10
5	3	3	2	36.37	36.389	2.4682	10
6	3	3	2	36.39	36.389	2.4669	10
7	-2	4	4	36.44	36.452	2.4636	12
8	-5	0	2	36.52	36.52	2.4584	10
9	-3	3	5	36.57	36.569	2.4551	12
10	-5	1	2	37.24	37.248	2.4125	14
11	-5	1	3	37.3	37.29	2.4087	45
12	-5	1	3	37.31	37.29	2.4081	49
13	2	1	5	37.35	37.364	2.4056	65
14	2	1	5	37.37	37.364	2.4044	73
15	4	1	2	37.39	37.407	2.4031	80
16	4	1	2	37.41	37.407	2.4019	86
17	-5	0	4	37.45	37.49	2.3994	96
18	-5	0	4	37.48	37.49	2.3976	100
19	-5	0	4	37.5	37.49	2.3963	100
20	-2	1	7	37.53	37.565	2.3945	99

Peak No.	H	K	L	2Th(Found)	2Th(Calcd)	d-sp. A	Rel. Int.
21	-2	1	7	37.56	37.565	2.3927	93
22	-2	1	7	37.6	37.565	2.3902	87
23	-4	1	6	37.67	37.674	2.3859	60
24	-1	5	2	37.72	37.724	2.3829	32
25	0	5	3	39.86	39.867	2.2597	11
26	1	2	6	40	40.02	2.2522	11
27	-4	2	7	43.41	43.412	2.0828	10
28	-5	3	1	43.44	43.434	2.0814	14
29	0	6	0	43.47	43.489	2.0801	19
30	0	6	0	43.51	43.489	2.0783	29
31	-5	3	4	43.54	43.545	2.0769	34
32	2	7	8	77.28	77.285	1.2336	26
33	1	10	1	77.32	77.328	1.233	18
34	6	5	6	81.04	81.015	1.1856	12
35	8	4	3	81.07	81.089	1.1852	17
36	2	2	12	81.1	81.096	1.1848	21
37	-9	4	0	81.12	81.123	1.1846	22
38	-7	4	12	81.15	81.153	1.1842	23
39	-9	3	10	81.18	81.187	1.1839	24
40	-9	3	10	81.21	81.187	1.1835	23
41	7	7	1	81.23	81.256	1.1833	22
42	7	7	1	81.26	81.256	1.1829	20
43	7	7	1	81.29	81.256	1.1826	19
44	6	6	5	81.33	81.326	1.1821	17
45	-2	2	14	81.36	81.363	1.1817	15
46	-10	3	5	81.4	81.389	1.1812	11

Table 4: The average crystallite sizes of complexes (3) and (4)

Sample No.	Lattice parameters				Volume in ($Å^3$)	Crystal size *D* (nm)	Crystal System
	a (Å)	b (Å)	c (Å)	β[º]			
3	12.210	12.508	17.045	115.16	2356.24	62.20	Monoclinic
4	12.322	12.476	17.081	110.72	2455.91	53.21	Monoclinic

Table 5:- The inhibition zone (mm) of the ligand and its metal complexes on microorganisms at different Concentrations

Comp. No.	**250 µg / mL**		**200 µg / mL**	
	A. niger	***E. coli***	***A. niger***	***E. coli***
DMSO	0	0	0	0
(Tetracycline)	0	28	0	20
Amphotricene B	23	0	17	0
1	19	22	12	8
2	14	19	9	5
3	20	19	10	4
4	28	24	18	9
5	18	15	8	6
6	17	16	7	7
7	18	20	8	5
8	18	14	8	6
9	22	17	10	8
10	28	18	12	8
11	29	19	11	9
12	20	14	9	7

Tables Captions:

Table 1:- UV-Vis. spectra of the ligand (H_2L) and its metal complexes.

Table 2: Miller indices (*hkl*), observed, calculated 2θ angles, *d* values, and relative intensities for complex (3)

Table 3: Miller indices (*hkl*), observed, calculated 2θ angles, *d* values, and relative intensities for complex (4)

Table 4: The average crystallite sizes of complexes (3) and (4).

Table 5:- The inhibition zone (mm) of the ligand and its metal complexes on microorganisms at different Concentrations

Graphical Abstract:

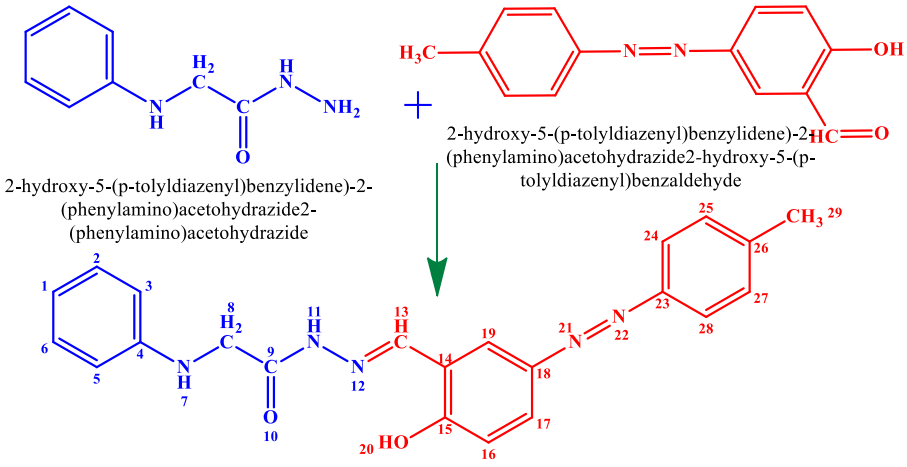

Figures:

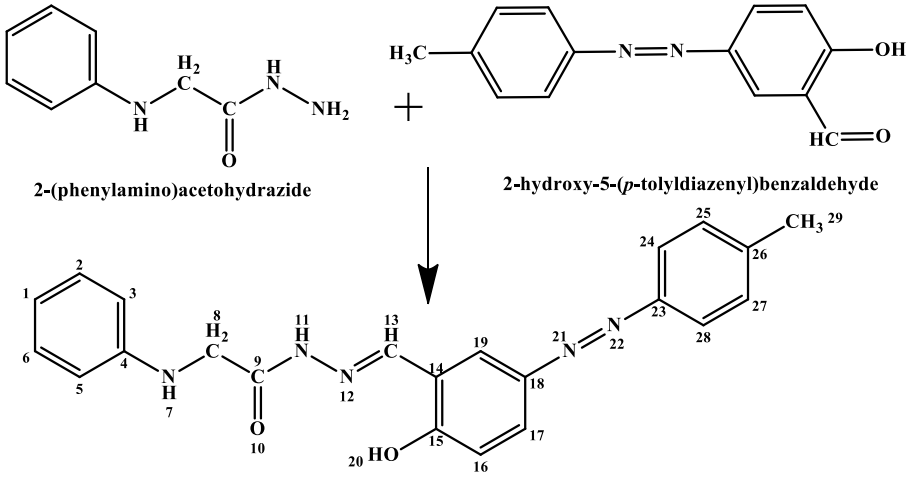

Scheme 1. Preparation of Ligand, 2-hydroxy-5-(*p*-tolyldiazenyl) benzylidene)-2-(phenylamino)acetohydrazide

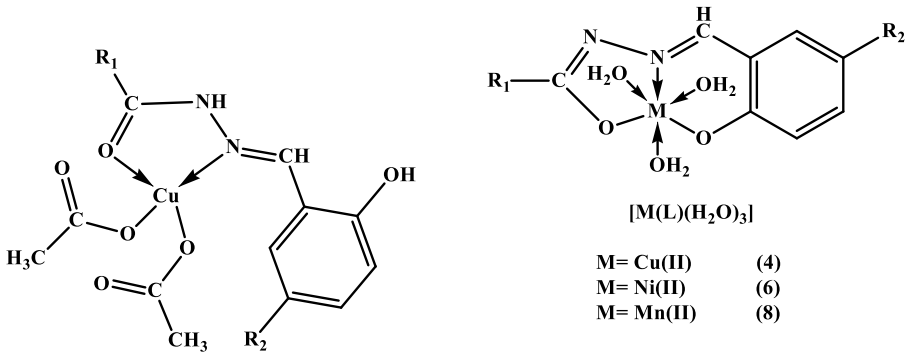

Fig. 1: Structure representation of Cu(II), Ni(II), Mn(II) and Zn(II) complexes (2, 4, 6, 8, 12)

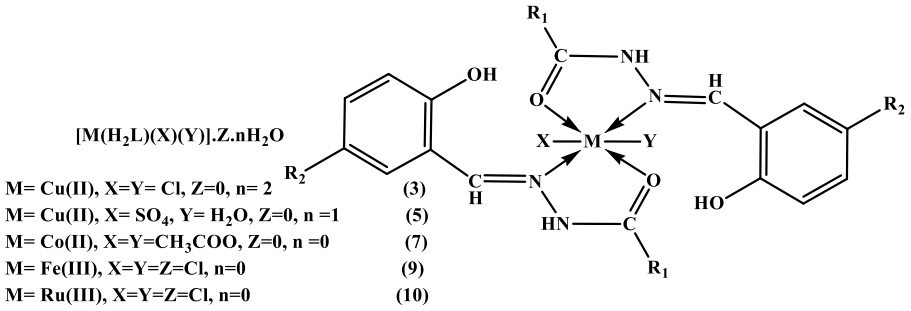

Fig. 2: Structure representation of Cu(II), Co(II) Fe(III) and Ru(III) complexes (3, 5, 7, 9, 10)

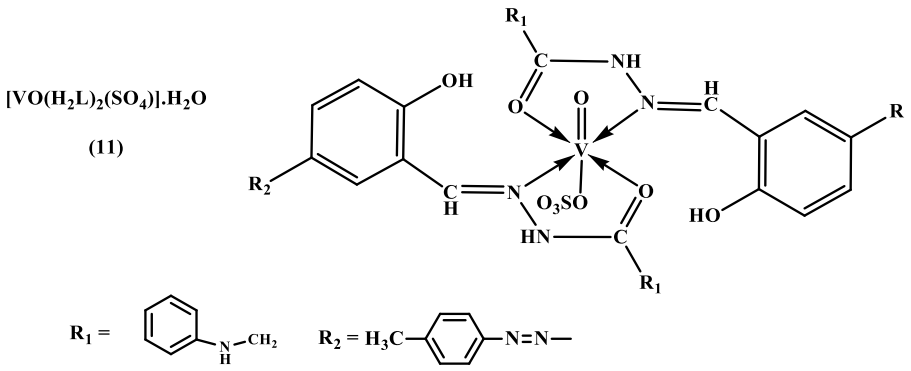

Fig. 3: Structure representation of VO(II) complex (11)

تحضير ودراسات طيفية وفعالية ضد الجراثيم لمعقدات المعادن مع الآزو–اسيتوهيدرازيد

أحمد الحكيمي [٢،١], محمد شقدوفه [٤،٣], أشواق الخولاني [٢], سمير عثمان [٥], فتحي السيد [٦],

إبراهيم الحجري[٢،١], محمد وهبة [٤]

١– كلية العلوم , قسم الكيمياء , جامعة القصيم , المملكة العربية السعودية

٢– كلية العلوم , قسم الكيمياء , جامعة اب , اليمن

٣– كلية العلوم والآداب , قسم الكيمياء , الخليص , جامعة جدة, المملكة العربية السعودية

٤– المعهد القومي للبحوث , الدقي , جمهورية مصر العربية

٥– كلية العلوم , قسم الفيزياء , جامعة اب , اليمن

٦– كلية العلوم , قسم الكيمياء , جامعة المنوفية , جمهورية مصر العربية

ملخص البحث. حضرت مترابطات جديدة من الآزو عن طريق تكاثف ٢–هيدروكسي –٥– (بارا توليلديازينيل) بنزالدهيد مع ٢– (فينيل امينو) اسيتو هيدرازيد وبواسطة التحليل المعدني المحدد لنسب الكربون والهيدروجين والنيتروجين بالإضافة الي التحليل الطيفي (الاشعة فوق البنفسجية وتحت الحمراء والرنين النووي المغناطيسي المعتمد على بروتون الهيدروجين او النظير الكربون ١٣) حدد الشكل العام للمترابط. التحاليل الطيفية وضحت تصرف المترابط بشكل ثنائي السن المتعادل او ثلاثي السن ثنائي القاعدية في المعقدات المحضرة حيث يرتبط العنصر الفلزي من خلال ذرة الاكسجين في مجموعة الكربونيل ونيتروجين مجموعة الازوميثين وأحيانا مع اكسجين مجموعة الفينول السالبة، الاشكال المتكونة توزعت بين ثمانية السطوح المشوهة والمربع المستوي. اجريت دراسات اشعة اكس على مسحوق المعقدين (٣) و (٤) لتوضيح الشكل البلوري. أظهرت الدراسات البيولوجية قدرة المركبات المحضرة على تثبيط النمو البكتيري والفطري حيث اظهر المعقد (١١) اعلى نسبة تثبيط فطري بينما اظهر المعقد (٤) اعلى نسبة تثبيط بكتيري من بين كل المركبات المدروسة.

مفتاح الكلمات : آزوهيدرازون , اسيتوهيدرازيد , معقدات معدنية , فعالية بيولوجية